

NOTICE CONCERNING COPYRIGHT RESTRICTIONS

This document may contain copyrighted materials. These materials have been made available for use in research, teaching, and private study, but may not be used for any commercial purpose. Users may not otherwise copy, reproduce, retransmit, distribute, publish, commercially exploit or otherwise transfer any material.

The copyright law of the United States (Title 17, United States Code) governs the making of photocopies or other reproductions of copyrighted material.

Under certain conditions specified in the law, libraries and archives are authorized to furnish a photocopy or other reproduction. One of these specific conditions is that the photocopy or reproduction is not to be "used for any purpose other than private study, scholarship, or research." If a user makes a request for, or later uses, a photocopy or reproduction for purposes in excess of "fair use," that user may be liable for copyright infringement.

This institution reserves the right to refuse to accept a copying order if, in its judgment, fulfillment of the order would involve violation of copyright law.

5958

ABSTRACT

As a result of the studies conducted by the Seismology Group in the Geophysics Department of CICESE in the Cerro Prieto Geothermal Field, the Geology Department of CFE requested that similar studies be conducted in the geothermal field of Los Azufres, Michoacán.

In order to establish approximate values for the rate of seismicity, to determine the advisability of installing a permanent observation network and to select the most suitable sites for recording on the basis of low noise levels, continuous local and regional seismicity observations were made during a period of 9 months. Based on the results of previous results in similar areas, observations focused on the analysis of the statistical properties of the seismic signals when they crossed production zones in comparison to zones where little is known regarding the existence of reservoirs.

To study the anelastic properties and heterogeneity of the local vertical structure of each of the sites observed by the local network of seismographic stations, we have analyzed the train of compressional waves (P) and the train of shear waves (S) produced by regional seismic events that occurred during the observation period of the present study (July 4, 1980 to March 23, 1981) and were located by the Red Sísmica Mexicana de Apertura Continental (RESMAC) and published in the monthly bulletins of the Instituto de Investigaciones en Matemáticas Aplicadas y en Sistemas (IIMAS) of UNAM.

The arrival times of 26 seismic events (whose typical seismograms are shown in figure 4) at each of the local network stations (figure 1), located in the well zone of the Tejamaniles Module, were read for P-waves. The arrival times of the S-waves are generally difficult to identify, because of the presence of multiple arrivals in the form of a complex wave, which masks the first arrivals of the train of S-waves. The seismic signal arrival azimuths at the network stations vary within a range of 70 to 270, thus making it possible to observe anomalies in arrival time and variance of the S-wave train over a 10-second window time, which in most cases is the duration of the dominant train of S-waves. This estimate of the power spectrum of the dominant wave-train was obtained for each of the 26 seismic signals as a function of the

azimuth arrival at each of the observation points.

Variance in the dominant train of compressional waves (P) could not be estimated qualitatively, chiefly because the train is severely attenuated at all the network observation points. Variance generally increases as the observation window time increases; the first arrivals of the train during a 5-second window time are strongly attenuated, which indicates that the energy cone involved is strongly attenuated along the ray paths at the minimum run time. These observations are discussed in greater detail in the report, Informe GEO-8201.

Estimated attenuation as a function of relative changes in the power of a particular signal observed at each station in relation to the average power of the signal over the entire network was compared to the apparent velocities of the P-wave in relation to the Agua Fria station (AGF) in the center of the graben of the Tejamaniles Module and at all the azimuths involved.

The distribution of the apparent velocities of the P-wave as a function of the azimuth when it crosses the Tejamaniles Module, figure 2, shows a tendency toward minimum values in two dips at azimuths of 160° and 230° with a relative intermediate maximum value of 200°. The apparent velocities decrease dramatically in each direction, from 2.5 km/s to velocities below 1 km/s, respectively, which indicates the existence of an anomalous body of low density and rigidity in the region between the AGF, P11 and P07 stations, associated with the complex structure between the graben controlled by the San Alejo-Agua Fria Faults, the PuenteCillos-Los Azufres Faults and the El Viejón Fault system.

The relative arrival times of events propagated through the network in the direction of azimuth $180^\circ \pm 30$ (figure 2) have been projected onto a north-south profile, with the relative values for time and distance. The average slope of the total values provide us with an estimate of the propagation velocity of the signal at the base of the anomalous structure under the network of 2.84 km/s.

Local attenuation at each of the observation points as a function of the

azimuth is shown in figure 3. The arrangement of the graphs applies to the geometry of the network and it may be noted that the signals are attenuated locally (at the Agua Fría station, AGF) by a factor greater than 4 at an azimuth of 240° increasing up to an average factor of 10 at an azimuth of 100°, which is consistent with the anomalies in the apparent velocities in this range of azimuths. In the same figure, it may be observed that the zone of anomalies attenuation is limited to the region located to the north of the Puenteillas-Los Azufres Fault and to azimuths of 240° to 90° as indicated in figure 1. The P11 station, for example, recorded local attenuation on the same order as the average values for the entire network, as may be seen in the seismograms and in the set of typical seismograms in figure 4, which clearly show how the attenuation of the wave-train is lower than that observed in the other stations, in contrast to the severe attenuation throughout the seismogram of the AGF station.

The P03 station in the extreme northwest of the zone under study exhibits local attenuation (figure 3) increasing from a factor of 9 to 10 in both directions from the azimuth of 160°; in contrast, the AJL station, 2 kilometers to the south of P03, does not show the same tendency, but has a constant attenuation no less than a factor of 2 for azimuths of 190°, which is consistent with the attenuation in the wave-train in the related seismogram. In the LCH station, located to the extreme southeast of the zone under study, a local effect of relative amplification is recorded, which increases up to more than 20 for azimuths greater than 190° and a constant value of almost 0 for lower azimuths, as may be observed in the distribution of its attenuation values.

The above results suggest the presence of an anomalous body of low rigidity and density, with high attenuation of shear waves limited to the region between the San Alejo and Puenteillas-Los Azufres Faults and quite probably associated with the tensile stresses that control the Tejamaniles and Agua Fría graben, which is indicated in figure 1 and extends in an east-west direction in alignment with the direction of the Agua Fría Fault.

Some lines of evidence on the surface extension of this anomalous body are provided by the two events closest to the geothermal area, one 5 km from the closest station (P03) in an east-west direction, as shown in the 3-D projection, where its hypocenter and epicenter have been plotted. An examination of the seismograms

in figure 5 and the paths at each of the stations shows that the records in the AGF, LCH and P11 stations present strong attenuation both in the train of P-waves and S-waves (P and S-wave energy graphs, figure 6a).

The other event located by RESMAC 55 km northwest of the zone and reaching the field at an average azimuth of 74° for all the stations shows strong attenuation in the signal arriving at the AGF, P11 and AJL stations, as indicated in the P and S-wave energy content graph in figure 6b. These results are helpful in delineating the limits of this anomalous body, which is outlined in figure 1.

The lines of evidence on the depth of this anomalous body are provided by an analysis of the average dominant frequency recorded in the power of the S-wave train as a function of the azimuth, which is shown in figure 7. If we interpret this frequency as "resonance" of the wave-train in the anomalous body due to the high impedance of velocity of the matrix, we see that peak resonance occurs at a frequency of 3.8 hz at an azimuth of 230° and decreases to 1.0 hz for an azimuth of 160°, which suggests that the anomalous body should be aligned in this azimuth with gradual spreading in the matrix at lower azimuths. A quantitative description of the depth of this anomalous body is beyond the scope of the analysis of observations discussed in the present study.

Local seismicity, in terms of typical tectonic events characterized by impulsive arrivals of the P and S-wave trains and gradual decline dominated by coda waves, is rare and almost null inside the zone covered by the network; in its place, "typical" seismic events of type "B", described as typical of volcanic seismicity in Japan, are observed.

The wave forms and frequencies (number of events per unit of time) that characterize seismicity in the neighboring areas around each of the network observation sites are gradually emerging arrivals that grow in amplitude without any clear indication of shear waves (S) and the total duration of the envelope measured over a signal length delimited by noise levels is, on the average, 2 seconds at the AGF station and on the same order at the other stations. Even though it is difficult to determine the geographic position and depth of focal points of seismic activity, it very probably occurs at shallow depths no greater than 2 kilometers. The distribution of such activity is quite possibly uniform in the hatched circles shown in figure 1a and associated with a

relaxation of stresses through increases or losses in the geothermal aquifer or reservoir pressures, that is, it should be associated with a relaxation of thermal stress, since the wave forms of the seismogram suggest that such stresses are produced by volumetric sources.

Table I shows the distribution of the number of events per unit of time observed during the recording period of this study. In this Table, we can see that the major seismic event is found in the zones surrounding the AJL, P07 and P03 stations with practically no activity in the areas surrounding the P11 and AGF stations. In the lower part of the Table, station coordinates, depth of bases and gains are given.

From the present study we may conclude that: the strong attenuation of the power spectrum of the S-wave train and the severe attenuation of the power spectrum of the P-wave train, by at least a factor of 4 in the case of the S train, the extremely low values of the apparent velocities through the network in reference to the AGF station, the effect of resonance dependent on the azimuth of the seismic arrival at the network and the nature of the local seismic events at the observation points indicate a relaxation of stresses due to pressure changes in the reservoirs, which suggests the presence of an anomalous body of low density and rigidity, whose geometric configuration is oriented along two preferential azimuths of 160° and 230° and extends in an east-west direction, quite possibly associated with reservoirs and geothermal reservoirs. The relaxation of cavity thermal stresses in this anomalous body are quite possibly associated with the migration of fluids toward and away from the reservoir.

LIST OF FIGURES

Fig. 1. 3-D Topography of the geothermal zone of Los Azufres, Michoacán, showing the location of recording sites with portable stations. The layout of the 6 stations encloses the Tejamaniles and Agua fría module. To the left, the hypocenter and epicenter of an earthquake that occurred 5 km west of the field are plotted and their seismograms are shown in Fig. 5.

Fig. 1a. Map of the geothermal zone of Los Azufres, Michoacán with the location of the network of portable stations. The hatched regions of various forms indicate the surface mapping of zones that are anomalous in seismic velocities and S-wave energy content. The hatched circles indicate the inferred

zones of local seismic activity.

Fig. 2. (left) Azimuth versus apparent velocity of the seismic signal when it crosses the Tejamaniles Module. The graph was constructed by comparing differences in arrival times and distances between the Agua Fria (AGF), LCH, P11, P07 and AJL stations. (right) North-south profile at an azimuth of 180° against relative arrival times of the signal for events arriving at an azimuth of $180^\circ \pm 30^\circ$. The slope of all the observations gives an average velocity of 2.84 km/s. The velocity between the P11 and AGF station, whose orientation coincides at an azimuth of 180° , is plotted in the upper section.

Fig. 3. Graphs of the azimuth of the arrival signal against an attenuation constant. The constant is calculated using Parceval's method for energy content. The arrangement of the graphs corresponds to the geometry of the network installed in the field. Zones in which the values of the constant are negative, indicating attenuation, may be observed.

Fig. 4. Six seismograms of a regional seismic event that occurred 348 km from the field and arrived at an azimuth of 195° . Strong attenuation in the amplitude of the S-wave packet in the AGF station may be observed, in addition to an increase in the period of the signal in station P11.

Fig. 5. Five seismograms of an event that occurred 5 km west of the field. The gain recorded at the AJL station was 6 dB greater than at the rest of the stations. Strong attenuation at the AGF and P11 stations may be observed. The graph for energy content of this event is shown in Fig. 6.

Fig. 6. (Left) distance covered by the seismic signal versus the calculation of energy content in the P and S-wave packet for the event that occurred 5 km west of the field. The stations have been projected onto an east-west profile. (right) Distance covered by the seismic signal versus the calculation of energy content in the P and S-wave packet for the event that occurred 55 km northwest of the field and arrived at an azimuth of 74° . The stations have been projected onto a profile in the direction of the azimuth of 74° . The scale of the vertical axis is logarithmic.

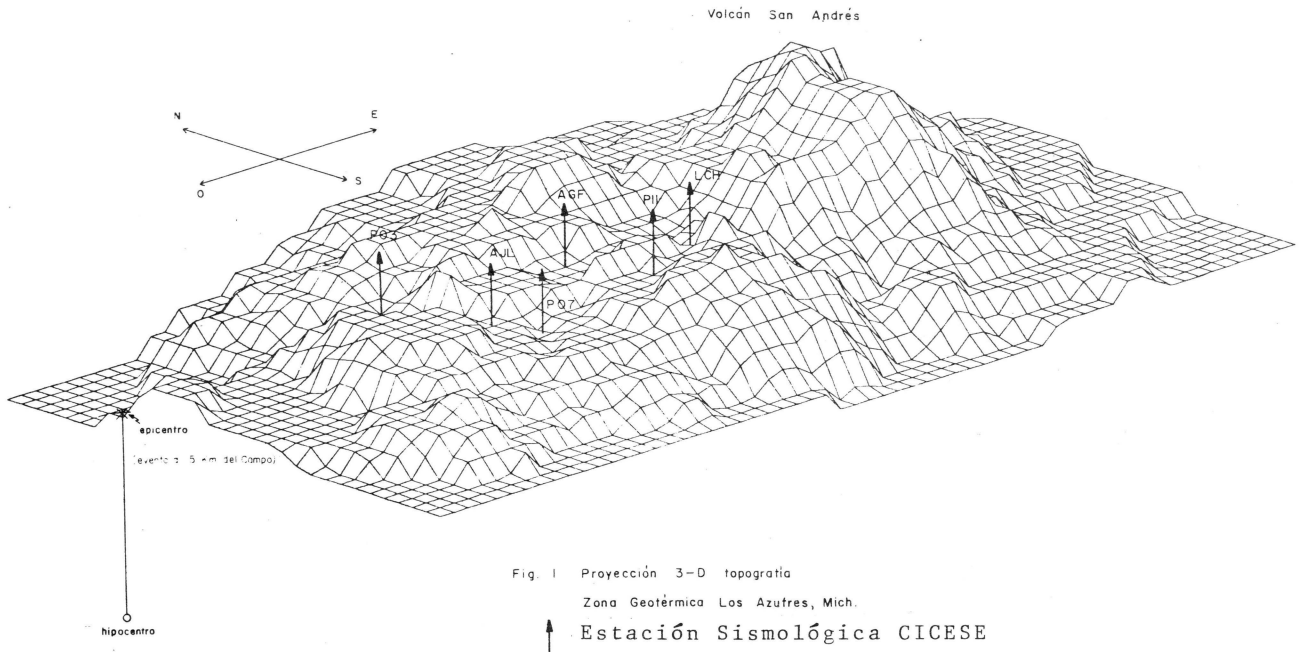
Fig. 7. Azimuth versus signal frequency for events occurring at an average distance of 350 km. Note the 2 declines in frequency at azimuths of 213° and 165° .

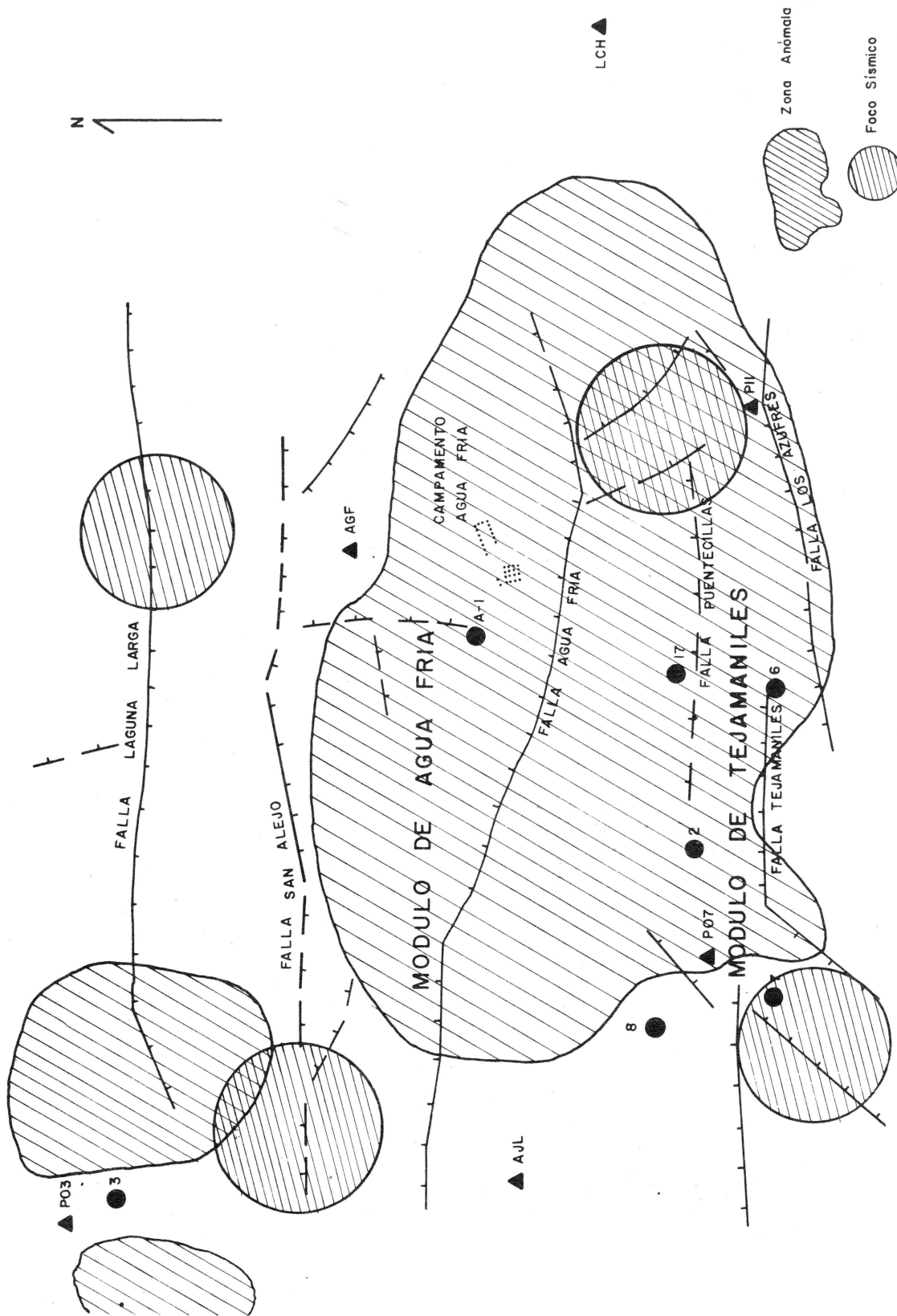
ganancia que el resto de estaciones. Puede observarse la fuerte atenuación en las estaciones AGF y P11. La gráfica de contenido de energía para este evento se da en la Fig. 6.

Fig. 6 (Izquierda) Distancia recorrida por la señal sísmica contra el cálculo de energía contenida en el paquete de ondas P y S, para el evento ocurrido a 5 kms. al oeste del campo. Las estaciones se han proyectado sobre un perfil Oeste-Este. (Derecha) Distancia recorrida por la señal sísmica contra el cálculo de energía

contenida en el paquete de ondas P y S, para el evento ocurrido a 55 kms al Noreste del Campo y arribando en un azimut de 74°. Las estaciones han sido proyectadas en un perfil en dirección a el azimut 74°. La escala en el eje vertical es logarítmica.

Fig. 7 Azimut contra frecuencia de la señal, para eventos ocurridos a distancia promedio de 350 kms. Obsérvense 2 decaimientos en frecuencia a los azimuts de 213° y 165°.





● POZOS C.F.E. ▲ ESTACIONES SISMOLOGICAS (CICESE) ARREGLO DE ESTACIONES
 ESC. 1:20 000

Fig. 1a

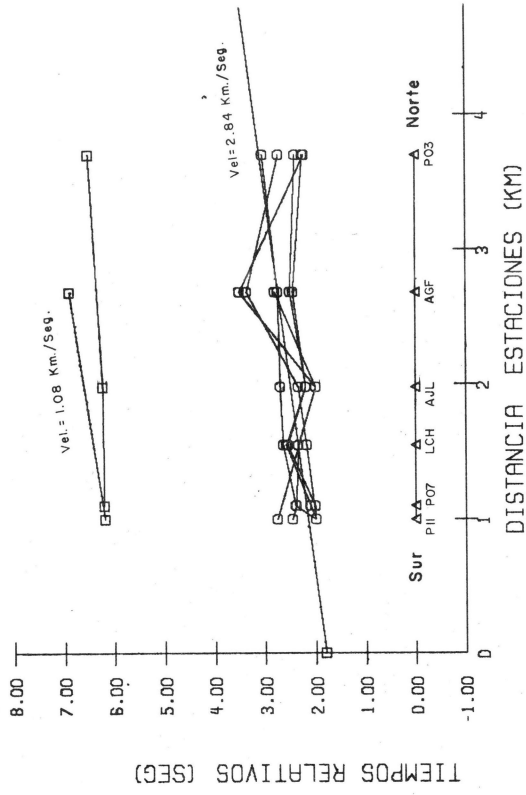
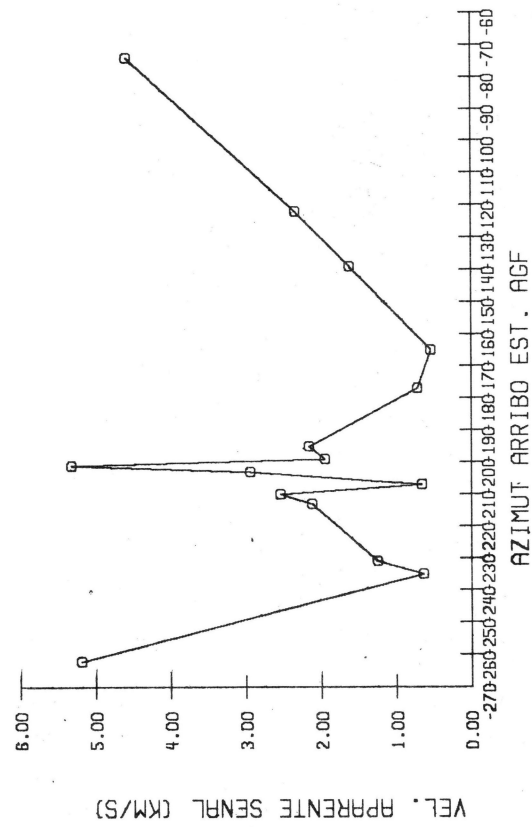
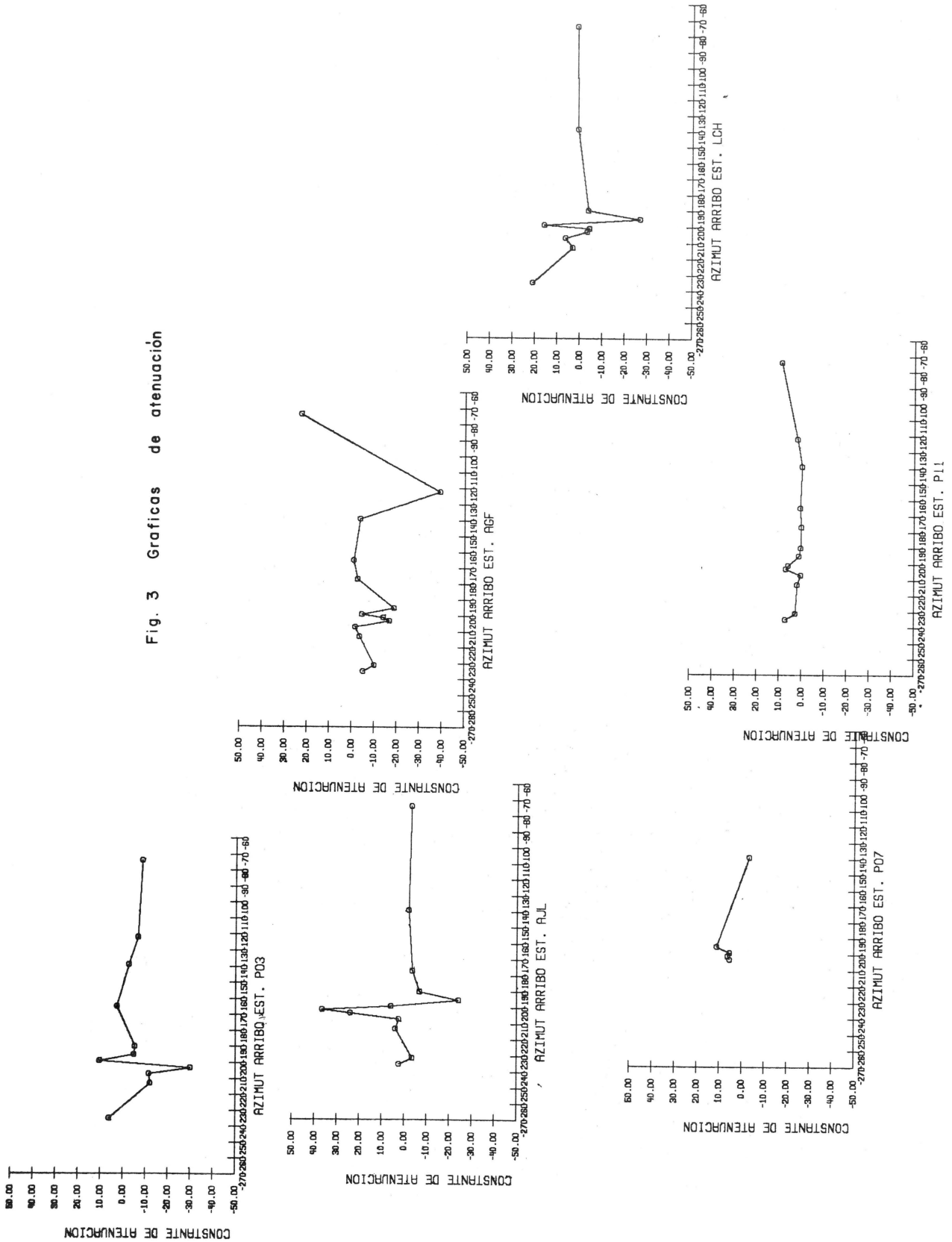


Fig. 2 Velocidades aparentes y tiempos relativos

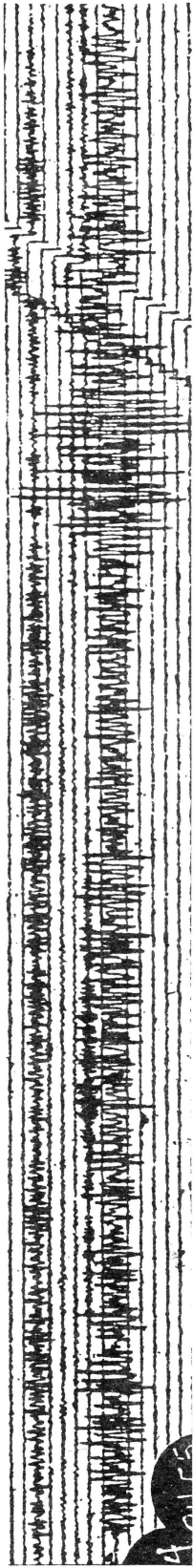
Fig. 3 Graficas de atenuación



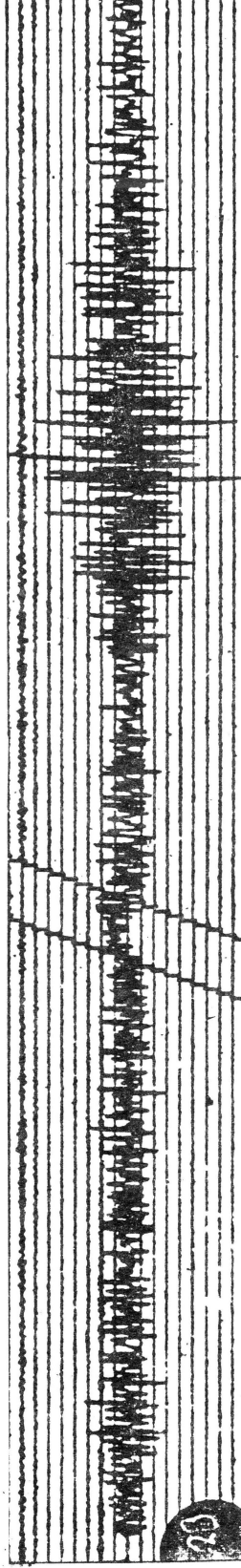
P11



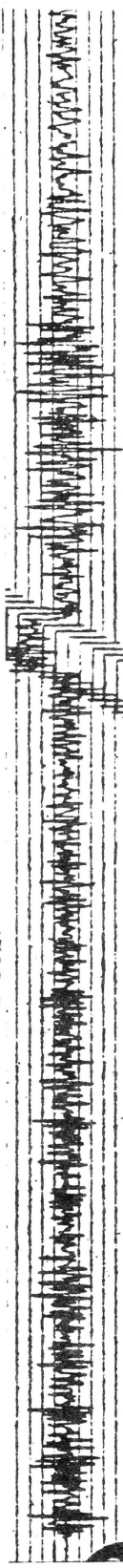
PO7



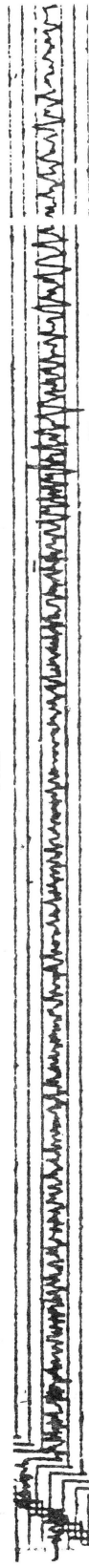
LCH



AJL



AGF



PO3

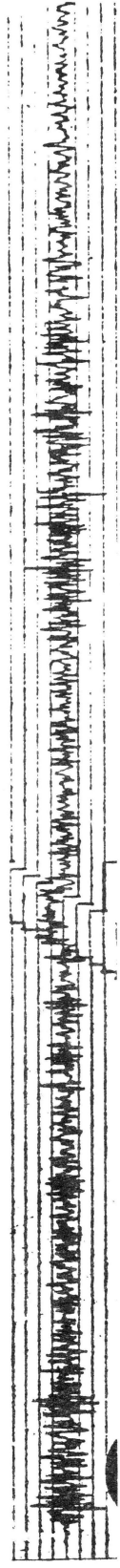


Fig. 4.- Sismo regional registrado en 6 estaciones de la Red.

Azimet arribo al Campo: 195°
Distancia recorrida: 348 Km.

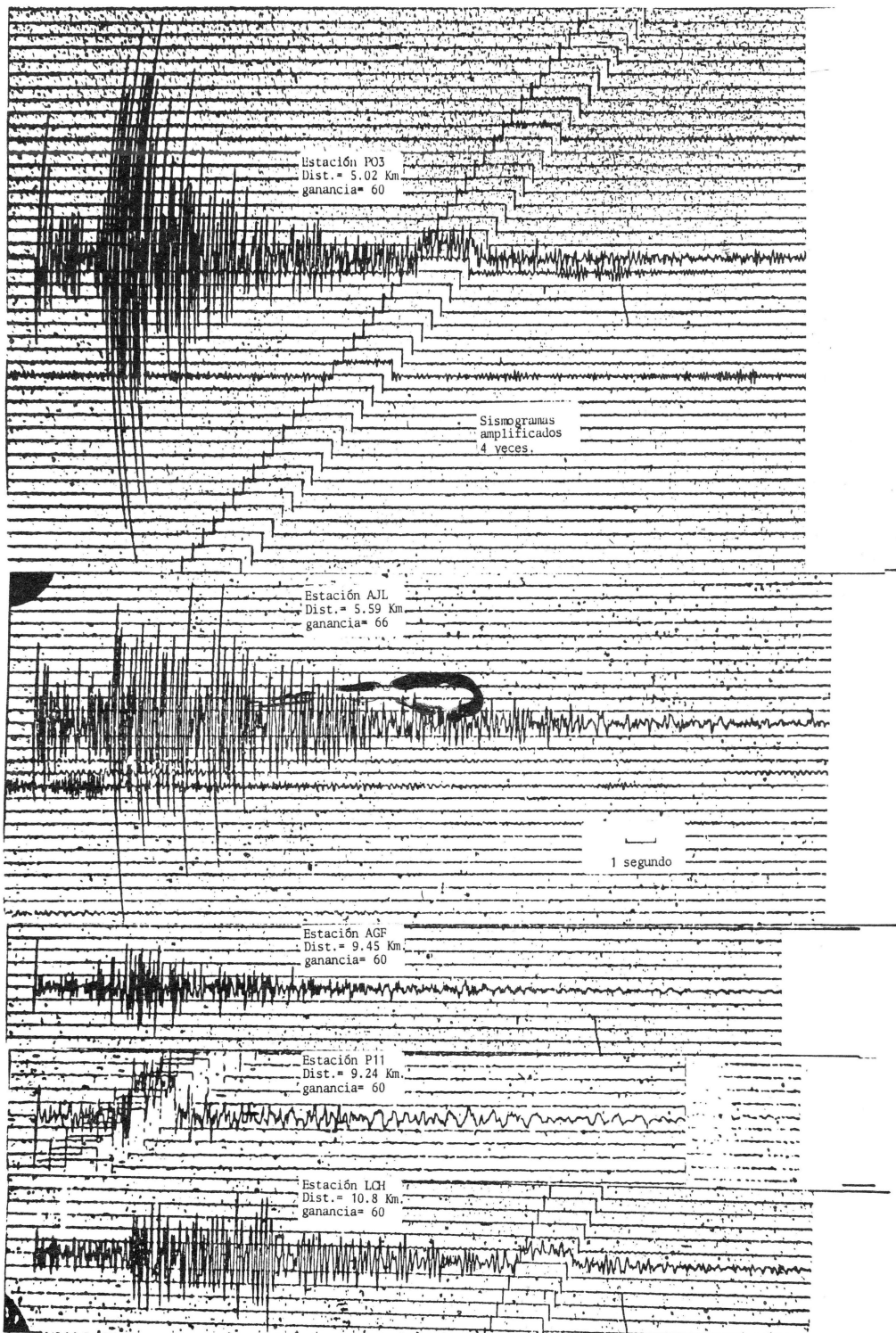


Fig. 5.- Sismogramas de evento sísmico ocurrido a 5 Km. al Oeste del Campo Geotérmico, como se grafica en la figura 1, proyección 3-D. Gráficas de contenido de energía, fases P y S para este evento, se muestran en la fig. 6a.

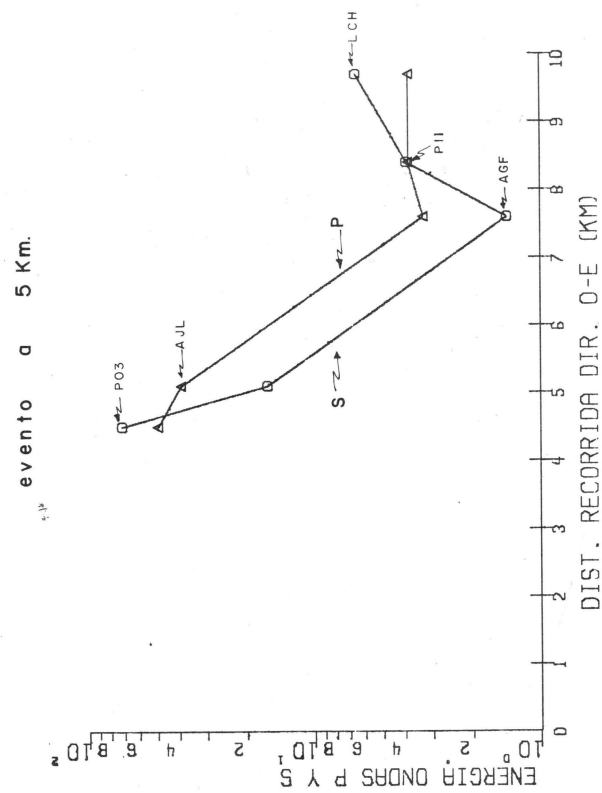
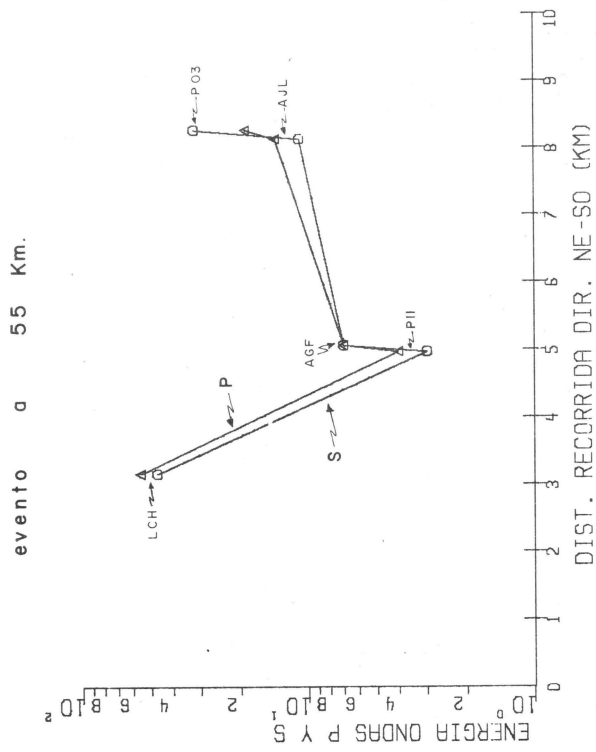


Fig. 6 Energía ondas P y S de 2 eventos cercanos.

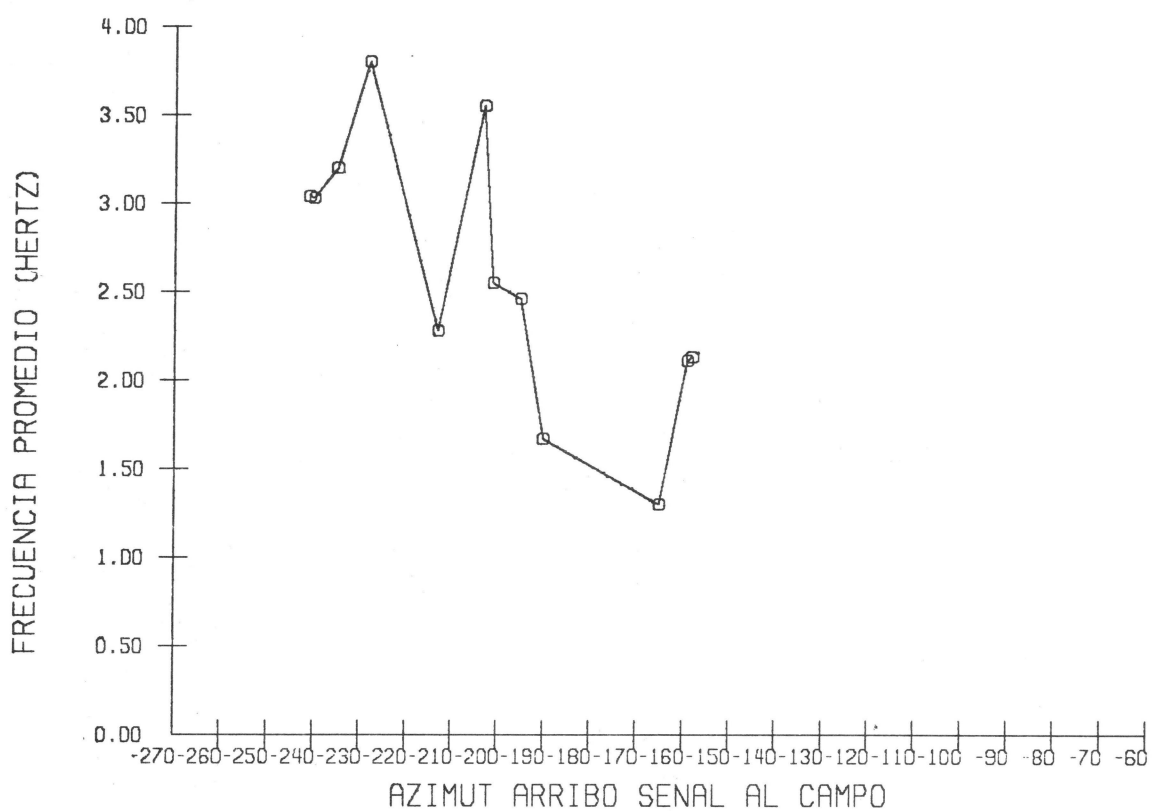


Fig. 7 Gráfica Azimut vs. Frecuencia de sismos
ocurridos a 350 Km. promedio.

Tabla I

ESTACION	N.E.R.	D.R.A.	D.R.T.	P.O.E.	I.A.D.	C.E.D.	D.N.O.E.
PO7	261	29	181	1.44	9.0	.049	20
AGF	148	21	155	0.95	7.0	.045	22
P11	98	21	129	0.75	4.6	.036	28
PO3	109	21	122	0.89	5.2	.042	24
AJL	174	13	113	1.53	13.38	.118	8
LCH	65	13	102	0.63	5.0	.049	20

Simbología:

N.E.R. = Numero de eventos registrados

D.R.A. = Días de registro de actividad

D.R.T. = Días de registro total

P.O.E. = Probabilidad de ocurrencia de 1 evento

I.A.D. = Indice de Actividad Diaria

C.E.D. = Cantidad de Evento por día.

D.N.O.E. = Dias necesarias para la ocurrencia de 1 evento.

ESTACION	SIGLA	COORDENADAS GEOGRAFICAS		PROF. BASES	GANANCIA
		LATITUD	LONGITUD		
POZO 7	PO7	19°46.86'	100°40.61'	3 metros	60 db.
AGUA FRIA	AGF	19°47.74'	100°39.49'	3 metros	60 db.
POZO 11	P11	19°46.79'	100°39.33'	3 metros	60 db.
POZO 3	PO3	19°48.30'	100°41.24'	3 metros	60 db.
AJOLOTES DE RUIZ	AJL	19°47.34'	100°41.13'	3 metros	60 db.
LLANO CHICO	LCH	19°47.14'	100°38.41'	3 metros	60 db.